ARTICLE OPEN

Check for updates

Electroacupuncture facilitates remote fear memory erasure via promoting perineuronal net degradation

Shuai-Wen Teng[1,2,4], Wen-Bo Guo[2,4], Bing-Feng Song[1], Yun-Zhang He[2], Ke-Yan Wang[2], Shi-Bin Gao[2], Wei Li[2] and Zhe-Yu Chen[1,2,3]✉

© The Author(s) 2025

Post-retrieval extinction has been effective in erasing recent pathological memories but has been shown failed in erasing remote memories. Pathological memories are often formed over the long term, therefore how to erase the remote pathological memory remains a long-lasting question. Here, we identified the increased perineuronal nets (PNNs) surrounding engram cells with memory being remote in the prelimbic cortex (PrL) which rigidify the remote memory from erasure. Microinjection of ChABC into PrL could facilitate remote memory erasure by degrading PNNs in post-retrieval extinction paradigm. In addition, electroacupuncture (EA) at Baihui (GV20) and Neiguan (PC 6) could degrade the PNNs in PrL by increasing the neuronal MMP-9 expression via BDNF-TrkB signaling, leading to the remote memory erasure under post-retrieval extinction condition. Finally, we found EA stimulation facilitated remote memory erasure led to increased overlap between fear and extinction cells in the PrL. Our data clarified the essential role of PNNs surrounding engram cell in preventing remote memory from erasure, and provided evidences of EA facilitates remote pathological memory erasure as a non-invasive therapeutic method.

Translational Psychiatry (2025)15:531 ; https://doi.org/10.1038/s41398-025-03789-3

INTRODUCTION

Pathological memory is harmful but difficult to treat, people may get posttraumatic stress disorder (PTSD) with the long-term stability of these memories [1, 2]. Among the most efficacious treatments for pathological memory are exposure-based therapies, during which a process called memory extinction is delivered by repeatedly presenting the conditioned stimulus (CS) in the absence of the unconditioned stimulus (US) [3–5]. In the context of extinction therapies, reconsolidation updating approaches called post-retrieval extinction paradigm have been proven effective to block fear memory spontaneous recovery which indicate fear memory erasure in rodents and humans [6, 7]. However, traumatic memories are oftentimes month-year old remote memories which are more stable than recent ones [8, 9]. Previous report found that post-retrieval extinction paradigm failed to erase remote memory whereas an HDAC2-targeting inhibitor administration restored the effect of post-retrieval extinction paradigm on memory erasure [10]. Our previous study found that the overlapping ensemble between fear cell and extinction cell was crucial for recent memory erasure which indicate the essential role of neuronal plasticity in memory erasure [11]. Hence, to investigate the effective non-invasive modality which could alter brain activity or connectivity to erase remote traumatic memory is demanding in the posttraumatic stress disorder (PTSD) treatment.

Electroacupuncture has shown potential benefit for a variety of mental health disorders including anxiety disorders [12]. The evidence of effectiveness of EA for PTSD has also been reported and further confirmed in a well-designed randomized controlled trial [13, 14]. The mechanism of the benefit effects of EA on fear memory attenuation might be related to restoring synaptic plasticity in amygdala and hippocampus through BDNF-TrkB and endocannabinoid signaling pathway [15, 16]. However, all these studies mainly focused on the short-term effect of EA on recent fear memory. Whether acupuncture could prevent extinguished remote fear memory recovery namely erasure is still unclear.

Perineuronal nets (PNNs) are a specialized type of extracellular matrix (ECM) that surround specific neuron populations throughout the central nervous system, which were involved in the regulation of neuronal functions such as excitability and neuronal communication [17–19]. The remodeling of PNNs by matrix metalloproteinases (MMPs) and ADAMTS proteins contributes in retaining long-term memories, as well as limiting the learning of new memories [20]. It's reported that degradation of PNNs by chondroitinase ABC (ChABC) in amygdala specifically rendered subsequently acquired fear or drug memories susceptible to erasure [21, 22]. Memory is stored in memory engram cells and is reshaped by modification of the engram cells [11, 23, 24]. However, the relationship between the engram cell of remote memory and PNNs is still unclear. What's more, whether EA could regulate PNNs remodeling to modify remote memory is still unclear. To answer these questions, by using activity-dependent neuronal-tagging technology, EA combined with immunofluorescence staining and western blot experiments, we identified the effectivenessand mechanism of acupuncture on remote fear memory erasure.

[1]Department of Anatomy and Neurobiology, Shandong Key Laboratory of Mental Disorders and Intelligent Control, School of Basic Medical Sciences and Qilu Hospital, Cheeloo College of Medicine, Shandong University, Jinan, Shandong 250012, P.R. China. [2]Research Center for Basic Medical Sciences, Qilu Hospital of Shandong University, No.107 Wenhua Xi Road, Cheeloo College of Medicine, Shandong University, Jinan, Shandong 250012, P.R. China. [3]State Key Laboratory for Innovation and Transformation of Luobing Theory, No.107 Wenhua Xi Road, Jinan, Shandong 250012, P.R. China. [4]These authors contributed equally: Shuai-Wen Teng, Wen-Bo Guo. ✉email: zheyuchen@sdu.edu.cn

Received: 11 March 2025 Revised: 24 October 2025 Accepted: 28 November 2025
Published online: 06 December 2025

MATERIALS AND METHODS

Mice

All animal experiments were conducted in accordance with protocols approved by the Institutional Animal Care and Use Committee (IACUC) of Shandong University (ECSBMSSDU2021-2-111) and complied with the National Institutes of Health (NIH) Guide for the Care and Use of Laboratory Animals. Mice were housed in a temperature- and humidity-controlled environment under a 12 h light/dark cycle, with ad libitum access to standard laboratory pelleted chow and water.The following transgenic mouse strains were obtained from The Jackson Laboratory:c-fos:tTA transgenic mice (B6.Cg-Tg(Fos-tTA, Fos-EGFP*)1Mmay/J; Stock No. 018306). TRE:H2B-GFP transgenic mice (Tg(tetO-HIST1H2BJ/GFP)47Efu/J; Stock No. 005104). Additionally, male C57BL/6 J mice used in this study were purchased from Beijing Vital River Laboratory Animal Technology Co., Ltd. All mice were 8 weeks old at the start of the experiments, with a body weight of 23–25 g. Animals were allocated to experimental groups randomly and investigators were blinded to the group allocation during the experiment. Animals may be excluded only if they meet objectively verifiable conditions (e.g., death from non-experimental causes, technical errors during procedures, or biologically significant abnormalities).

Auditory fear conditioning

Mice underwent auditory fear conditioning (AFC) in a 25 cm × 25 cm × 25 cm fear conditioning chamber (Context A) equipped with an electrifiable grid floor connected to a shock generator, an ambient light source, and a speaker embedded in the chamber wall for auditory stimuli delivery. The chamber was thoroughly cleaned with ethanol before each trial, and all stimulus presentations were computer-controlled using specific software (Freezing, Panlab). Before conditioning, mice were habituated in the chamber for 3 min without any stimuli. The AFC protocol consisted of three tone (CS)–footshock (US) pairings, where the conditioned stimulus (CS) was a 30-s continuous tone (3 kHz, 80 dB), and the unconditioned stimulus (US) was a 0.75 mA footshock lasting 1 s, delivered at the end of each CS presentation. Each CS-US pairing was separated by a 120-s inter-trial interval (ITI). Following the final shock, mice remained in the chamber for an additional 2 min before being returned to their home cages.

Retrieval

Twenty-four hours after AFC, mice underwent the retrieval test in Context B, a novel chamber distinct from Context A in floor texture, color, shape, and odor. Mice were first habituated to Context B for 3 min. A single CS (20 s tone) was presented, followed by a 60 s rest period. Afterward, mice were returned to their home cages for 30 min before extinction training.

Extinction training

Extinction training was conducted in Context B. Mice were first habituated in the chamber for 3 min. They then received 39 tone-alone (CS, 20 s) presentations, with an ITI of 20 s.

Extinction trials were divided into four phases (Ext#1, Ext#2, Ext#3, Ext#4) based on the freezing response: Ext#1, Ext#2, and Ext#3: Each phase represents the average freezing response during the first 10 trials (total of 30 trials). Ext#4: Represents the average freezing response during the last 9 trials.

Extinction memory test (EM)

The extinction memory (EM) test assessed the retention of extinction learning. Mice were placed in Context B and habituated for 3 min before testing. They then received 4 tone-alone (CS, 20 s) presentations, with an ITI of 30 s.

Spontaneous recovery test (SR)

The spontaneous recovery (SR) test measured the recovery of fear responses following extinction. Two weeks after the EM test, mice were re-exposed to 4 tone-alone (CS, 20 s) presentations, with an ITI of 30 s, in Context B.

In all processes, the freezing was measured by a high-sensitivity weight transducer (load cell unit) which could record and analyze the animal movement intensity. The freezing level was scored during each experimental phase by the software (Freezing, Panlab).

Electroacupuncture (EA) procedure

Mice underwent EA treatment under 1.5–2% isoflurane anesthesia using sterile acupuncture needles (0.25 mm × 13 mm) for stimulation. The EA parameters were set to a 3 mA current intensity in a dense-sparse wave (DSW) mode, where the dense wave frequency was 10 Hz, and the sparse wave frequency was one-fifth of the dense wave frequency. The waves alternated with the sparse wave applied for 5 s, followed by the dense wave for 10 s, for a total EA session duration of 30 min. Acupuncture points included Baihui (GV20) (AP: −2 mm; ML: 0 mm), located on the intersection point of the midline and the line connecting the apexes of both ears, where the needle was inserted obliquely 2–3 mm into the scalp; Shenting (GV24) (AP: + 1.5 mm; ML: 0 mm), located on the intersection point of the coronal and sagittal sutures,positioned anterior to the bregma, approximately 2 mm superior to the interocular line, with the needle inserted obliquely 1–2 mm into the scalp; and Neiguan (PC6), found on the palmar midline of the forelimb, approximately 2 mm proximal to the wrist crease, where the needle was inserted obliquely 1.5–2 mm into the subcutaneous tissue. For the sham EA group, mice underwent the same procedures as the EA group, except no electrical stimulation was applied.

Immunofluorescence

Mice were euthanized by intraperitoneal injection of an overdose of pentobarbital sodium (Sagatal, RWD Life Science, Shenzhen, China), followed by transcardial perfusion with 4% paraformaldehyde (PFA). The brains were carefully dissected and post-fixed in 4% PFA at 4 °C for 24 h. Coronal brain sections (40 μm thick) were obtained using a vibratome (VT1200S, Leica, Germany). For immunofluorescence staining, sections were initially incubated in a blocking solution to prevent non-specific binding: 5% bovine serum albumin (BSA) in PBS with 0.3% Triton X-100 for WFA staining and 10% donkey serum in PBS with 0.4% Triton X-100 for other stains, both at room temperature for 2 h. Subsequently, the sections were incubated overnight at 4 °C with primary antibodies, including biotinylated Wisteria floribunda agglutinin (WFA, 1:500, L1516, Sigma), MMP-9 (1:500, ab38898, Abcam), NeuN (1:1000, 94403 s, Cell Signaling), and Iba1 (1:500, ab283319, Abcam). The next day, sections were incubated with secondary antibodies for 2 h at room temperature in the dark, including Streptavidin-R-Phycoerythrin (1:1000, 42250, Sigma), Streptavidin-FITC (1:1000, s3762, Sigma), Alexa Fluor™ 594-conjugated donkey anti-rabbit IgG (1:1000, A21207, Invitrogen), and Alexa Fluor™ 488-conjugated donkey anti-mouse IgG (1:1000, A21202, Invitrogen). Between each incubation step, sections were washed three times with PBS for 10 min each. Finally, the stained sections were mounted with DAPI-containing mounting medium and coverslipped. Multiple images were captured at 20x objective (pixel size 0.65 um) using a Zeiss LSM880 confocal microscope (Zeiss, Germany) at Translational Medicine Core Facility of Shandong University.

Western blot

Tissue blocks were collected and homogenized using a magnetic homogenizer with TX buffer (200 μL per 10 mg tissue) and 50–60 mg magnetic beads. The homogenate was centrifuged at 15,000 g for 20 min at 4 °C, and the supernatant was collected, with 6–7 μL reserved for protein quantification, while the remaining sample was either aliquoted and stored at −20 °C or mixed with loading buffer for Western blot analysis. Protein concentration was determined using the BCA Protein Assay Kit (Pierce BCA Protein Assay Kit, 23225, Thermo Fisher Scientific), and after normalization, 4× LDS Sample Buffer was added to the protein samples, mixed thoroughly, and heated at 95 °C for 5 min. The samples were then cooled and subjected to SDS-PAGE using a rapid gel preparation kit (Epizyme Biotech, PG113), followed by protein transfer onto a PVDF membrane. The membrane was blocked in 5% BSA for 1 h at room temperature and subsequently incubated overnight at 4 °C with primary antibodies, including MMP-9 (1:1000, ab38898, Abcam), BDNF (1:1000, ab108319, Abcam), and β-Actin (1:1000, sc-47778, Santa Cruz). After primary antibody incubation, the membrane was washed three times with 0.1% TBST. Secondary antibody incubation was performed by incubating the membrane at room temperature for 1 h with Goat Anti-Mouse IgG, H&L Chain-Specific Peroxidase Conjugate (1:5000, 401215, Sigma) or Peroxidase AffiniPure™ Goat Anti-Rabbit IgG (H + L) (1:5000, 111-035-003, Jackson-HRP), both diluted in 5% BSA. After three washes with 0.1% TBST, detection was carried out using enhanced chemiluminescence (ECL). Protein band densities were quantified using ImageJ software.

Stereotactic surgery and drug microinjections

To facilitate subsequent drug injections, guide cannulas were implanted into targeted brain regions with precision. Mice were anesthetized with 2% isoflurane and fixed in a stereotaxic apparatus (RWD Life Science).

A midline incision was made on the scalp to expose the skull, and a small hole was drilled at the PrL coordinates (AP: + 1.94 mm, ML: ±0.50 mm, DV: −2.2 mm). The guide cannula was secured 0.2 mm above PrL (DV: −2.0 mm) to prevent direct tissue damage. After surgery, mice were returned to their home cages and allowed to recover for two weeks before further experimentation. ChABC (Sigma-Aldrich, C3667) was dissolved in filtered 0.1 M PBS to a final injection concentration of 200 U/mL. ChABC, K252a (dissolved in 10% DMSO, 25 μm, Calbiochem, 420297) and SB-3CT (dissolved in 10% DMSO, 1 mg/ml, Selleck, S7430) were microinfused into PrL via the guide cannula. Microinjections were performed at a rate of 50 nl/min, delivering 300 nL per hemisphere into the PrL via PE20 tubing to a microsyringe driven by a microinfusion pump (KD Science, KDS310) [25]. After injection, the needle was left in place for 2–5 min to minimize reflux and ensure proper diffusion.

Activity-dependent cell labeling

To label the engram cells, we crossed c-fos:tTA transgenic mice with TRE:H2B-GFP transgenic mice and subjected the double transgenic mice to AFC. Alternatively, we injected AAV9-c-fos:tTA (BrainVTA; titer, 5.65×10^{12} vg/mL) and AAV9-TRE-mCherry (BrainVTA; titer, 5.34×10^{12} vg/mL) into wild-type (WT) mice for engram cell labeling. The double transgenic mice were maintained on a Dox-containing diet (40 mg/kg) from birth, while WT mice were placed on a Dox-containing diet two weeks prior to surgery. The mice were then removed from Dox for 24 h to open a window for fear memory engram labeling in context A. Following this, the animals were exposed to context A for fear conditioning, and the Dox diet was resumed immediately after AFC training.

Cell counting

To quantify the number of c-Fos$^+$, H2B-GFP$^+$, or mCherry$^+$ positive cells, we analyzed five 40 μm-thick coronal sections spaced at 120 μm intervals spanning the prelimbic cortex (PrL; Bregma 1.54 mm to Bregma 2.10 mm) in all experiments. The number of c-Fos$^+$, GFP$^+$, or mCherry$^+$ positive neurons was counted using NIH ImageJ, and the area of the PrL in each section was calculated. Overlap was determined by the ratio of (mCherry$^+$c-Fos$^+$/DAPI$^+$), while (c-Fos$^+$/DAPI$^+$) x (mCherry$^+$/DAPI$^+$) was calculated as the chance level of overlap in the PrL, as previously reported [11]. The area of PNNs was quantified by WFA staining, applying a positive threshold.

Real time (RT)-PCR

Total RNA from PrL tissue was isolated according to the Ultrapure RNA kit instructions. A 0.5 μg aliquot of each sample was treated with DNase to avoid DNA contamination and was then reversely transcribed using the RevertTra Ace qPCR RT Kit (TOYOBO, catalog FSQ-101). Primer sequences were as follows:

c-fos forward primer, 5′ GGGAATGGTGAAGACCGTGT 3′ reverse primer,5 ′ CCGTTCCCTTCGGATTCTCC3′;

arc forward primer, 5′ GATCTTTCCTGCTGTGCCCT3′ reverse primer, 5′ CGCAACAAGGCCTACTCAGA3′;

bdnf forward primer, 5′ GCCTAGATCAAATGGAGCTTCT 3′ reverse primer, 5′ GCCGATATGTACTCCTGTTCTG 3′;

mmp9 forward primer, 5′ AAGGGTACAGCCTGTTCCTGGT 3′ reverse primer, 5′ CTGGATGCCGTCTATGTCGTCT 3′;

adamts4 forward primer, 5′ ATGGCCTCAATCCATCCCAG 3′ reverse primer, 5′ AAGCAGGGTTGGAATCTTTGC 3′;

adamts5 forward primer, 5′ GGAGCGAGGCCATTTACAAC 3′ reverse primer, 5′ CGTAGACAAGGTAGCCCACTTT 3′. The β-actin was selected as a control (forward, 5′ AGA GGG AAA TCG TGC GTG AC 3′ and reverse, 5′ CAT ACC CAG GAA GGA AGG CT 3′). RT-PCR was performed in a Cycler (MyiQ2, Bio-Rad) using SYBR green (Takara, DRR041A). The threshold cycle (Ct) for each sample was selected from the linear range and converted to an initial quantity by interpolation from a standard curve run on the same plate for each primer set. Each sample was analyzed in duplicate, and the mRNA levels were normalized to β-actin mRNA levels for each well using the $2^{-\Delta\Delta Ct}$ method.

MMP-9 enzyme activity test

The MMP Activity Assay Kit (Abcam, ab112146) employs a fluorescence resonance energy transfer (FRET)-quenched peptide as a generic MMP activity indicator. Following enzymatic cleavage by MMPs, fluorescence recovery was measured using a fluorescence microplate reader at excitation/emission wavelengths of 490 nm/525 nm, with results normalized to protein concentration (per μg protein).

Statistics

All sample sizes were determined based on paradigms used in previous similar studies [21, 26, 27]. Data were analyzed using GraphPad Prism 8.0 (GraphPad Software, San Diego, CA, USA) with Student's t-test, one-way or two-way ANOVA followed by Tukey's or Sidak's multiple comparisons test. Each point represents one sample. For experiments with a single factor and two or more groups, Student's t-test or one-way ANOVA was applied. For experiments involving multiple factors, a two-way ANOVA with interaction testing was used. All data are presented as the mean ± SEM, with statistical significance set at $p < 0.05$.

RESULTS

Increased PNNs surrounding engram cell at remote time point prevent remote memory erasure

Given the essential role of PNNs in memory storage and extinction within the central nervous system [21, 26], we first examined whether PNN formation is associated with memory engram cells. Mice were trained using an auditory fear conditioning paradigm, and the TetTag system, which we have previously employed [11, 27], was used to label the memory engram cell. We observed an increased presence of PNNs in the PrL but not in BLA and CeA in the 30 days' group post-training, compared with the group examined 1 day post-training (Fig. 1A-D; Figure S1). In addition, the number of engram cells surrounded by PNNs in the PrL also exhibited a significant increase in 30 days group compared with 1 day group (Fig. 1E, F).

We then investigated whether the increase in PNNs during remote memory formation contributes to blockage of remote memory erasure. A post-retrieval extinction paradigm was employed to target the erasure of remote memory. While the post-retrieval extinction paradigm was effective in erasing recent fear memory, it could not erase remote memory, which is indicated by the spontaneous fear recovery (Figure S2C, D). Microinjection of ChABC into the PrL one day prior to post-retrieval extinction paradigm was found to effectively degrade PNNs, as demonstrated by Wisteria floribunda agglutinin (WFA) staining (Figure S2A, B). Notably, degradation of PNNs in the PrL facilitated remote memory erasure without leading to an increase in spontaneous recovery of fear memory (Figure S2C-F). Interestingly, at the time of the SR test, the PNNs had already reformed, while degrading PNNs via administering ChABC 24 h before SR does not affect SR tests of original fear memory (Figure S3). Thus, these results suggest the crucial role of PNNs in the PrL during post-retrieval extinction period in blocking remote fear memory erasure.

EA induced remote memory erasure in a PNN dependent mechanism

Acupoint stimulation has been utilized in clinical treatment for various disorders including PTSD. However, the relationship between EA and the expression of PNNs in the PrL, as well as its role in fear memory erasure, remains unclear. To address this, we examined the effects of EA stimulation at Baihui (GV 20) alone, Baihui (GV 20) combined with Neiguan (PC 6), and Baihui (GV 20) combined with Neiguan (PC 6) on PNN degradation. 24 days after fear memory training, EA was initiated and lasted for 7 days. WFA staining was performed at the end of EA to assess the impact of EA on PNN degradation. Our results revealed that EA stimulation at Baihui (GV 20) combined with Neiguan (PC 6) significantly reduced the PNNs levels in the PrL (Figure S4). We then investigated whether EA stimulation at Baihui (GV 20) combined with Neiguan (PC 6) could facilitate the erasure of remote fear memory using the retrieval-extinction (R + E) paradigm. Our findings demonstrated that retrieval-extinction paradigm following 7 days of EA stimulation effectively erased remote fear memory, accompanied by decreasing PNN levels in the PrL as well as selectively reducing the PNNs levels surrounding engram cells rather than non-engram cells (Fig. 2).

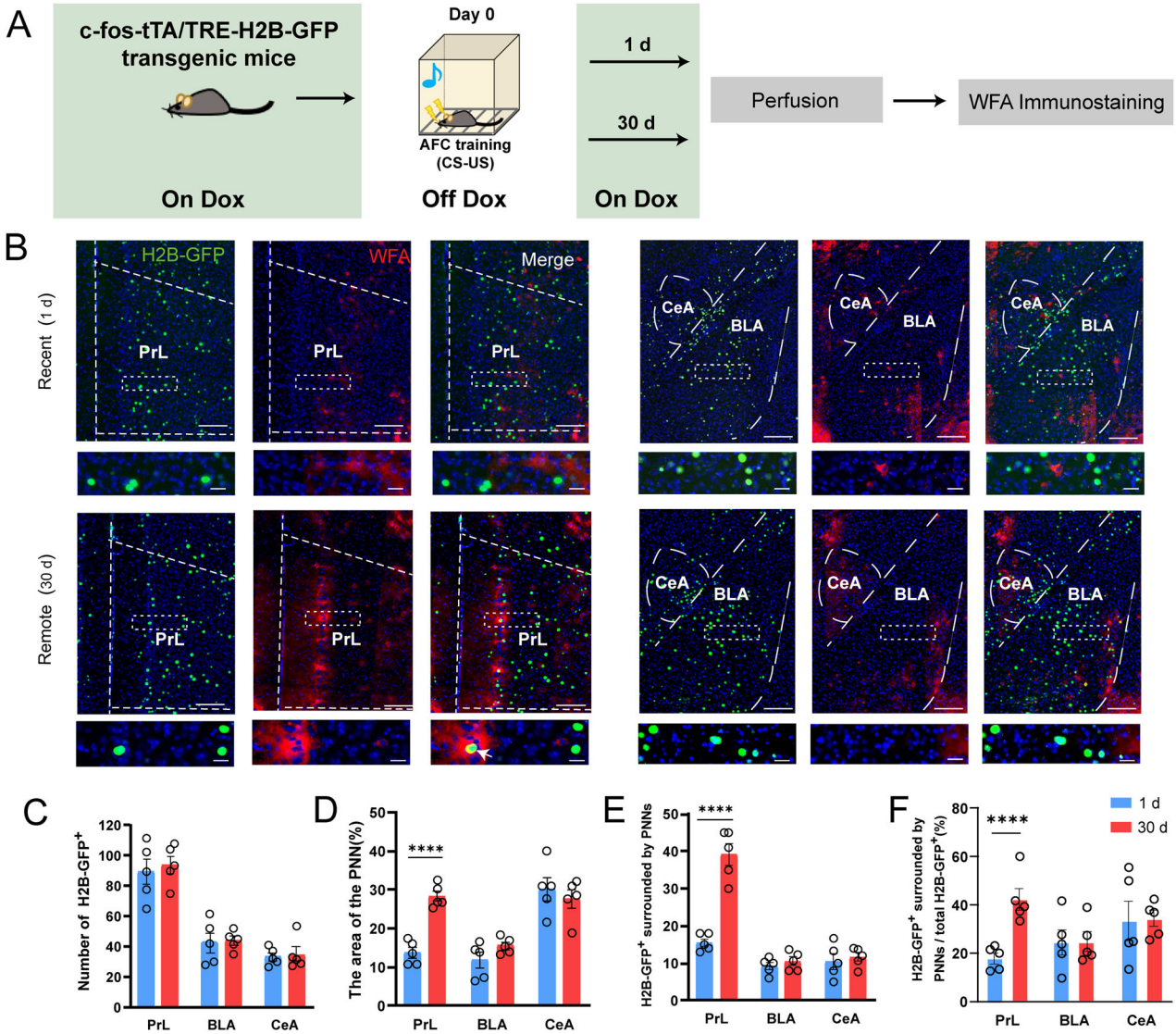


Fig. 1 The PNNs surrounding engram cells was increased in the PrL at a remote timepoint. A Labeling strategy of the inducible double transgenic TetTag mouse and the experimental design. **B** Representative images of H2B-GFP$^+$ (green) and c-Fos$^+$ (red) immunofluorescence in PrL, BLA and CeA.Scale bar, 200 μm (top), 20 μm (bottom). **C** Quantification of H2B-GFP+ cell number in PrL, BLA and CeA. **D** The levels of PNN expression in PrL, BLA and CeA (two-way ANOVA with Sidak's multiple comparisons test, ***$p < 0.001$; $n = 5$ animals per group including 3 females and 2 males). **E** Quantification of the number of c-Fos surrounded by PNNs in PrL, BLA and CeA. **F** Quantification of theratio of c-Fos surrounded by PNNs in PrL, BLA and CeA (two-way ANOVA with Sidak's multiple comparisons test, ***$p < 0.001$). Data are presented as mean ± SEM.

We next explored the mechanism underlying EA-induced PNN degradation. Our results showed that the mRNA levels of the immediate early genes c-fos and arc were elevated in the PrL following EA stimulation at Baihui (GV 20) combined with Neiguan (PC 6) (Fig. 3A, B). Additionally, the mRNA levels of BDNF and MMP9 were also increased in the PrL after this treatment, whereas adamts4 and admts5 showed no significant difference. Given the reported critical role of MMP9 in regulating PNN degradation [28, 29], we focused our subsequent investigations on this molecule. We found that the number of MMP9$^+$NeuN$^+$ cell was increased following EA stimulation at the Baihui (GV 20) combined with Neiguan (PC6) while the number of MMP9$^+$Iba1$^+$ cell showed no significant change (Fig. 3C-F), which suggested that EA stimulation could selectively increase the MMP9 expression in neurons. We next investigate the role of increased MMP9 expression in EA stimulation facilitated PNNs degradation and remote fear memory erasure. We found that microinjection of MMP inhibitor SB-3CT into PrL could block the EA stimulation facilitated remote memory erasure under the R + E paradigm compared with EA stimulation alone group. However, microinjection of ChABC combined with SB-3CT into PrL could erase the remote memory erasure as well (Fig. 4A, B), which suggests that MMP9 acts through PNNs in EA facilitated remote memory erasure. Furthermore, we observed an increase in the expression of BDNF and MMP9 in the EA+Vehicle, EA + SB-3CT, and EA + SB-3CT+ChABC groups, as determined by western blot analysis (Fig. 4C-F), which suggests that MMP9 enzyme activity rather than its expression levels play an essential role in mediating EA facilitated remote memory erasure. To confirm our results, we performed WFA immunostaining across these groups and found the decreased expression of PNNs in PrL following EA treatment was abolished by SB-3CT microinjection into PrL (Fig. 4G, H). The MMP-9 enzyme activity was also measured across these groups and we found that the MMP-9 enzyme activity was increased during RE and EM but not SR following EA treatment (Fig. 4I-K). In all, our results suggest that EA treatment could erase remote fear

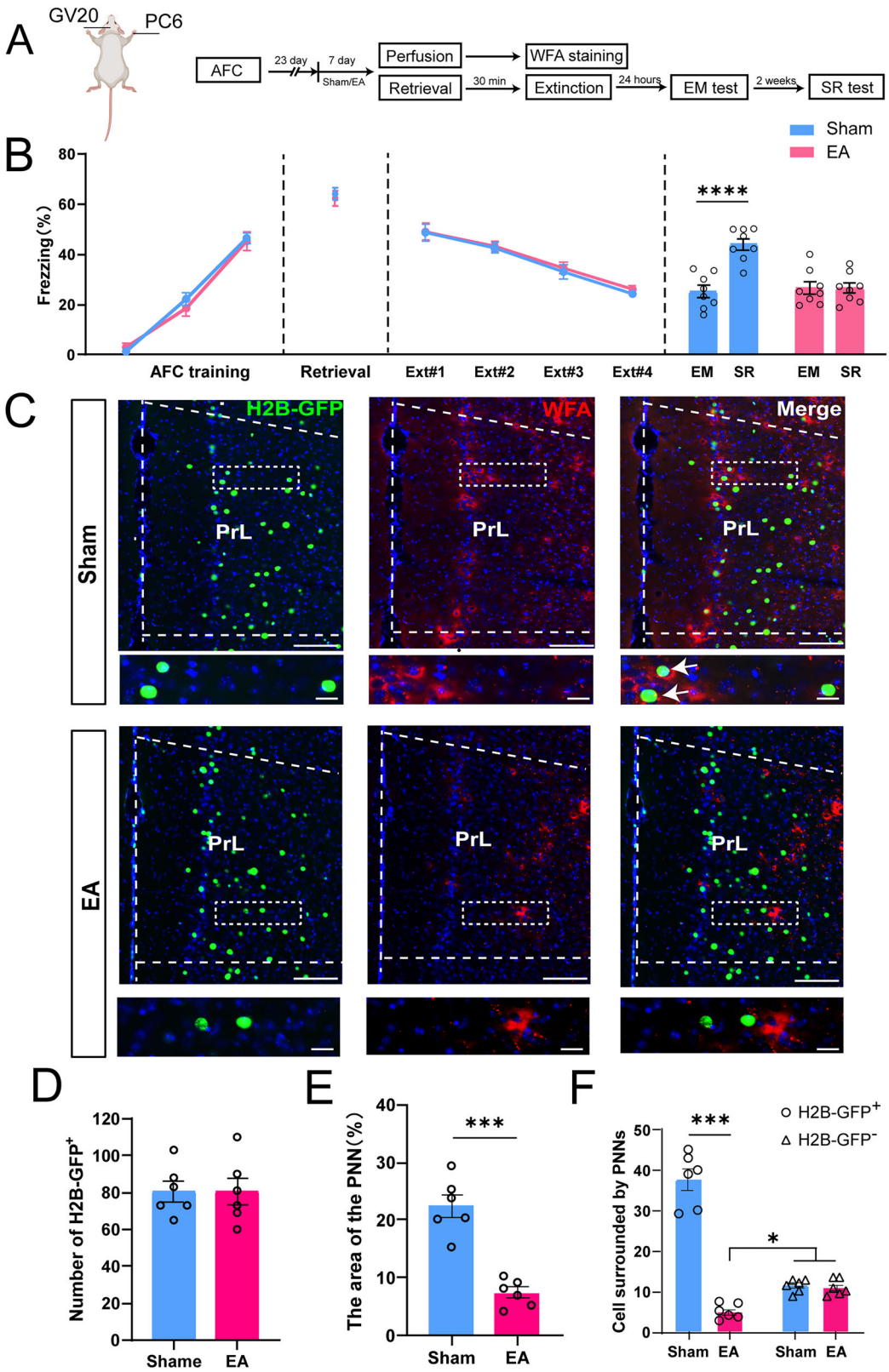


Fig. 2 Retrieval-extinction paradigm following 7 days of EA stimulation effectively erased remote fear memory. A Schematic of EA treatment, WFA staining following chABC microinjection into PrL and behavioral paradigm. **B** The freezing levels during conditioning, retrieval, extinction, EM test and SR test (RM two-way ANOVA with Sidak's multiple comparisons test, ****$p < 0.0001$; $n = 8$ animals per group including 4 females and 4 males). **C** Representative images of H2B-GFP (green) and WFA (Red) expression in the PrL. Scale bar, 200 μm (top), 20 μm (bottom). **D** The quantification of H2B-GFP$^+$ cells. **E** The levels of PNN in the PrL (unpaired t-test, ****$p < 0.0001$). **F** The cell number surrounded by PNNs expression of H2B-GFP$^+$ cells or H2B-GFP$^-$ cells in PrL (two-way ANOVA with Sidak's multiple comparisons test, *$p < 0.05$, ***$p < 0.0001$). Data are presented as mean ± SEM.

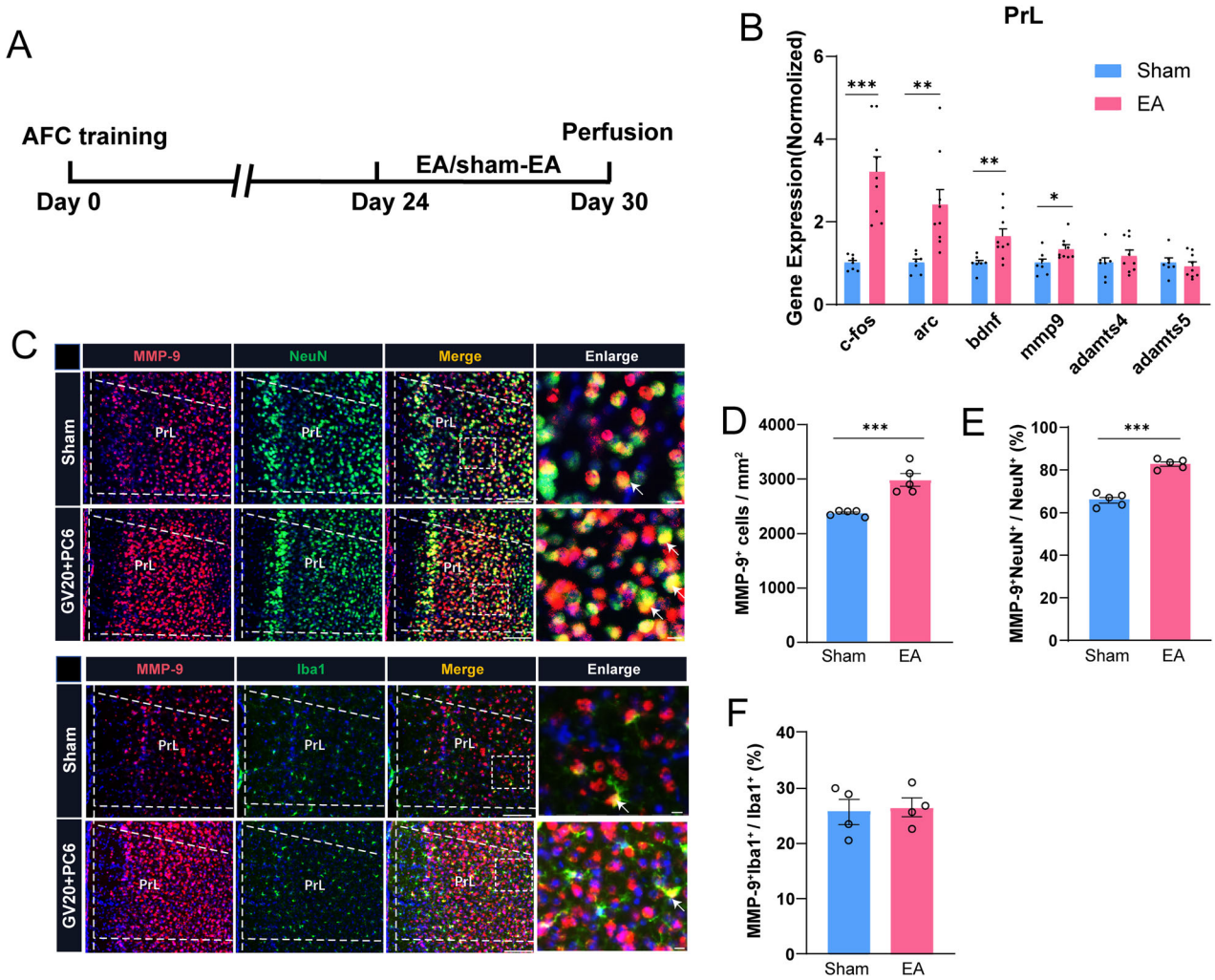


Fig. 3 EA induces increased MMP-9 expression in PrL neurons. A Schematic of EA treatments, WFA staining and behavioral paradigm. **B** The expression of c-fos, arc, bdnf, mmp9, adamts4 and adamts5 were verified by RT-PCR (two-way ANOVA with Sidak's multiple comparisons test, ***p < 0.001, **p < 0.005, *p < 0.05; n = 7 animals in Sham group, n = 9 animals in EA group). **C** Top: Representative images of MMP-9 (red) and NeuN (green) expression in the PrL. Scale bar, 200 μm (Top) and 20 μm (bottom). Bottom: Representative images of MMP-9 (red) and Iba1 (green) expression in the PrL. Scale bar, 200 μm (Top) and 20 μm (bottom). **D** Quantification of MMP-9 positive cell number in PrL (unpaired t-test, **p < 0.005; n = 4 animals per group). **E** Quantification of MMP-9^{+}NeuN^{+} cell number in PrL (unpaired t-test, ***p < 0.001; n = 4 animals per group). **F** Quantification of MMP-9+Iba1+ cell number in PrL. Data are presented as mean ± SEM.

memory under R + E paradigm via promoting PNN degradation in MMP9 dependent pathway.

Since it has been reported that the BDNF-TrkB signaling could regulate the expression of MMP9 [30]. We then investigate whether BDNF-TrkB signaling mediates EA induced increased MMP9 expression and remote memory erasure. We found that microinjection of TrkB inhibitor K252a into PrL could block the EA induced remote memory erasure under the R + E paradigm compared with EA alone group. However, microinjection of ChABC combined with K252a into PrL could restore the remote memory erasure (Fig. 5A, B). Additionally, we observed increased expression of BDNF in the EA + Vehicle, EA + K252a, and EA + K252a + ChABC groups, as determined by western blot analysis (Fig. 5C, D). However, K252a microinjection blocked the EA stimulated MMP9 expression increase (Fig. 5E, F), which suggest that BDNF-TrkB signaling mediates EA increased MMP9 expression. These findings were further corroborated by immunostaining experiments. We found K252a microinjection blocked EA induced PNN degradation in the PrL (Fig. 5G, H). In addition, the MMP-9 enzyme activity was also measured across these groups and we found that K252 treatment could effectively block the EA induced MMP-9 enzyme activity enhancement (Fig. 5I-K). Our results indicate that EA treatment facilitates the erasure of remote fear memory under the R + E paradigm by promoting BDNF-TrkB signaling, which increase MMP9 expression and drives the degradation of PNNs.

EA induced increased overlapping ensemble between fear and extinction cells in the PrL during remote memory erasure

Our previous study showed the increased overlapping ensembles between fear and extinction cells during recent memory erasure in the PrL and suggested that effective recent fear memory erasure is mediated by a rewriting of the original memory trace of fear toward one of safety [11]. We are wondering whether the overlapping ensemble between fear and extinction cells was increased with remote memory erasure. The virus based TetTag system, which we have previously employed [11], was used to label the memory engram cell during memory acquisition. The extinction ensemble was identified by the endogenous c-Fos immunostaining 90 min after the last extinction trial across different groups (Fig. 6A). Our results showed that the increased overlapping ensembles between fear and extinction cells in PrL during recent memory erasure, which was consistent with our previous study (Fig. 6B-E). However, we

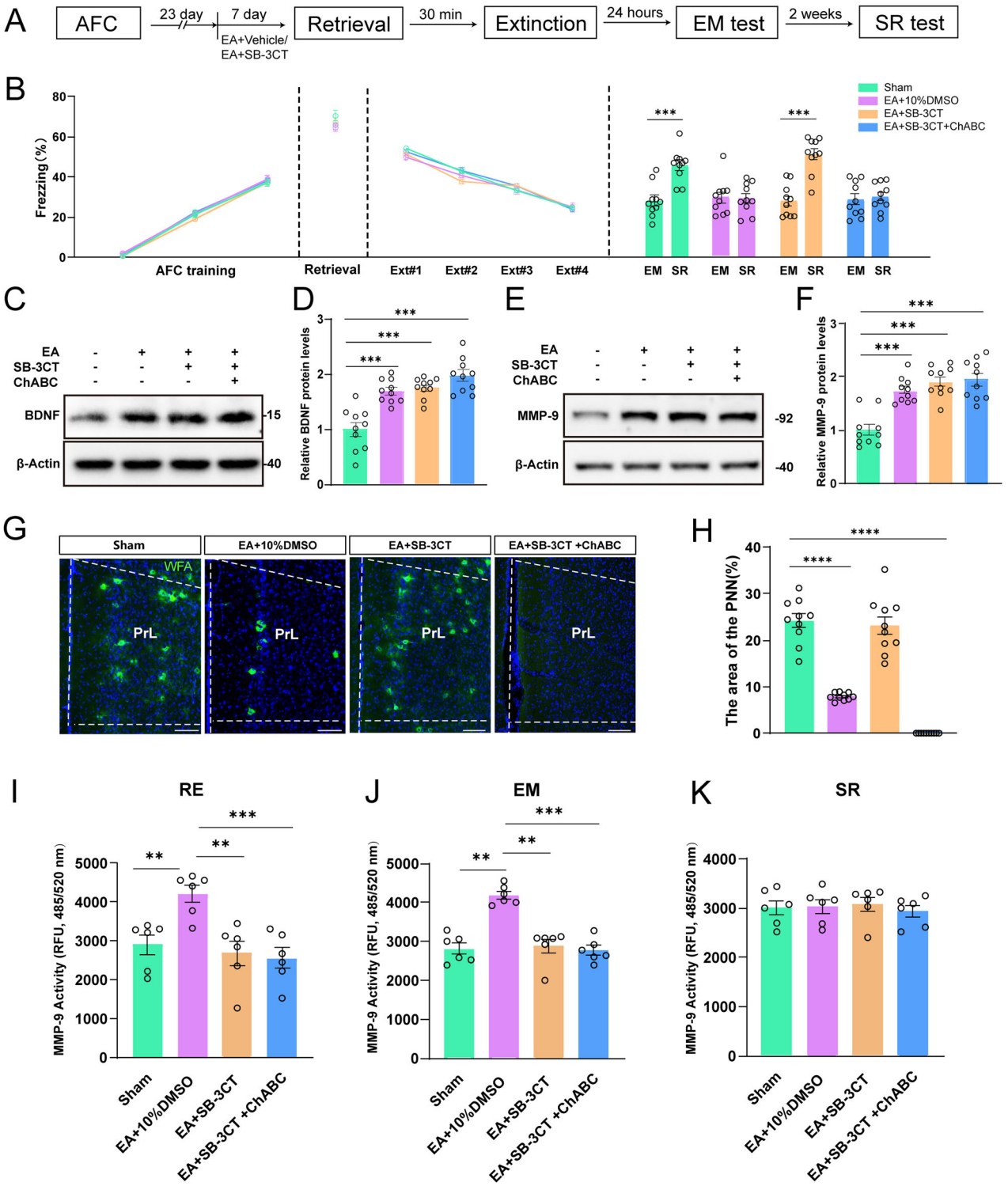


Fig. 4 EA treatment could erase remote fear memory under R + E paradigm via promoting PNN degradation in a MMP9 dependent pathway. A Schematic of EA treatments and behavioral paradigm. **B** The freezing levels during conditioning, retrieval, extinction, EM test and SR test (RM two-way ANOVA with Sidak's multiple comparisons test, ***p < 0.001; n = 10 animals per group including 5 females and 5 males). **C** Representative expression of BDNF in PrL by western blots. **D** Quantification of BDNF protein levels for western blot experiment (one way ANOVA with Turkey's post-hoc comparison, ***p <0.001). **E** Representative expression of MMP-9 in PrL by western blots. **F** Quantification of MMP-9 protein levels for western blot experiment (one way ANOVA with Turkey's post-hoc comparison, ***p <0.001). **G** Representative images of WFA (green) expression in the PrL. Scale bar, 200 μm. **H** Quantification of PNN levels in PrL for immunostaining experiment. (**I-K**) Quantification of MMP-9 enzyme activity during RE(I), EM (J) or SR (K) (one way ANOVA with Turkey's post-hoc comparison, **p <0.005, ***p <0.001). Data are presented as mean ± SEM.

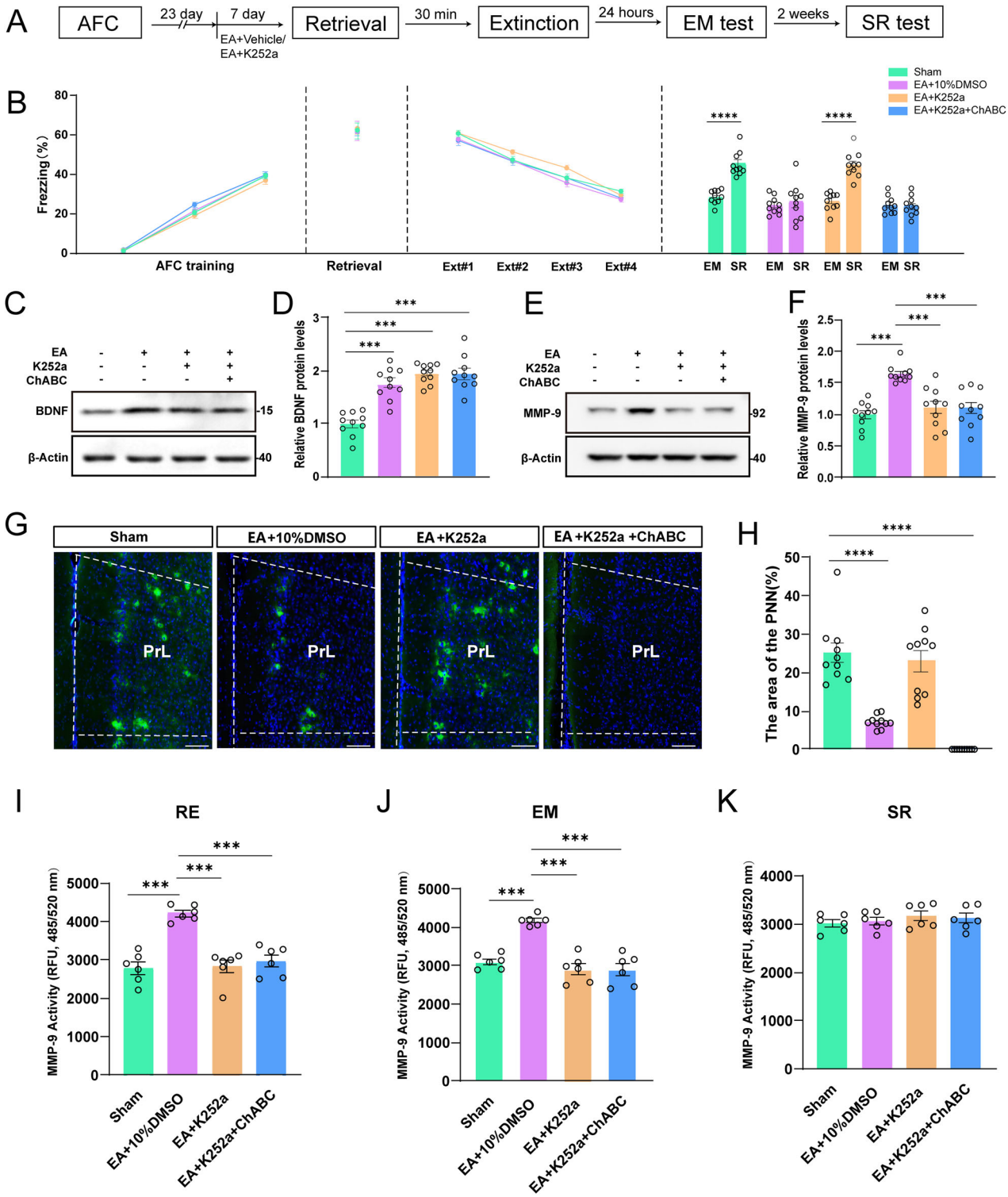


Fig. 5 EA induced remote memory erasure depends on BDNF-TrkB signaling. A Schematic of EA treatments and behavioral paradigm. **B** The freezing levels during conditioning, retrieval, extinction, EM test and SR test (RM two-way ANOVA with Sidak's multiple comparisons test, ***p < 0.001; n = 10 animals per group including 5 females and 5 males). **C** Representative expression of BDNF in PrL by western blots. **D** Quantification of BDNF protein levels for western blot experiment (one way ANOVA with Turkey's post-hoc comparison, ***p <0.001). **E** Representative expression of MMP-9 in PrL by western blots. **F** Quantification of MMP-9 protein levels for western blot experiment (one way ANOVA with Turkey's post-hoc comparison, ***p <0.001). **G** Representative images of WFA (green) expression in the PrL. Scale bar, 200 μm. **H** Quantification of PNN levels in PrL for immunostaining experiment. (**I-K**) Quantification of MMP-9 enzyme activity during RE(I), EM (J) or SR (K) (one way ANOVA with Turkey's post-hoc comparison, ***p <0.001). Data are presented as mean ± SEM.

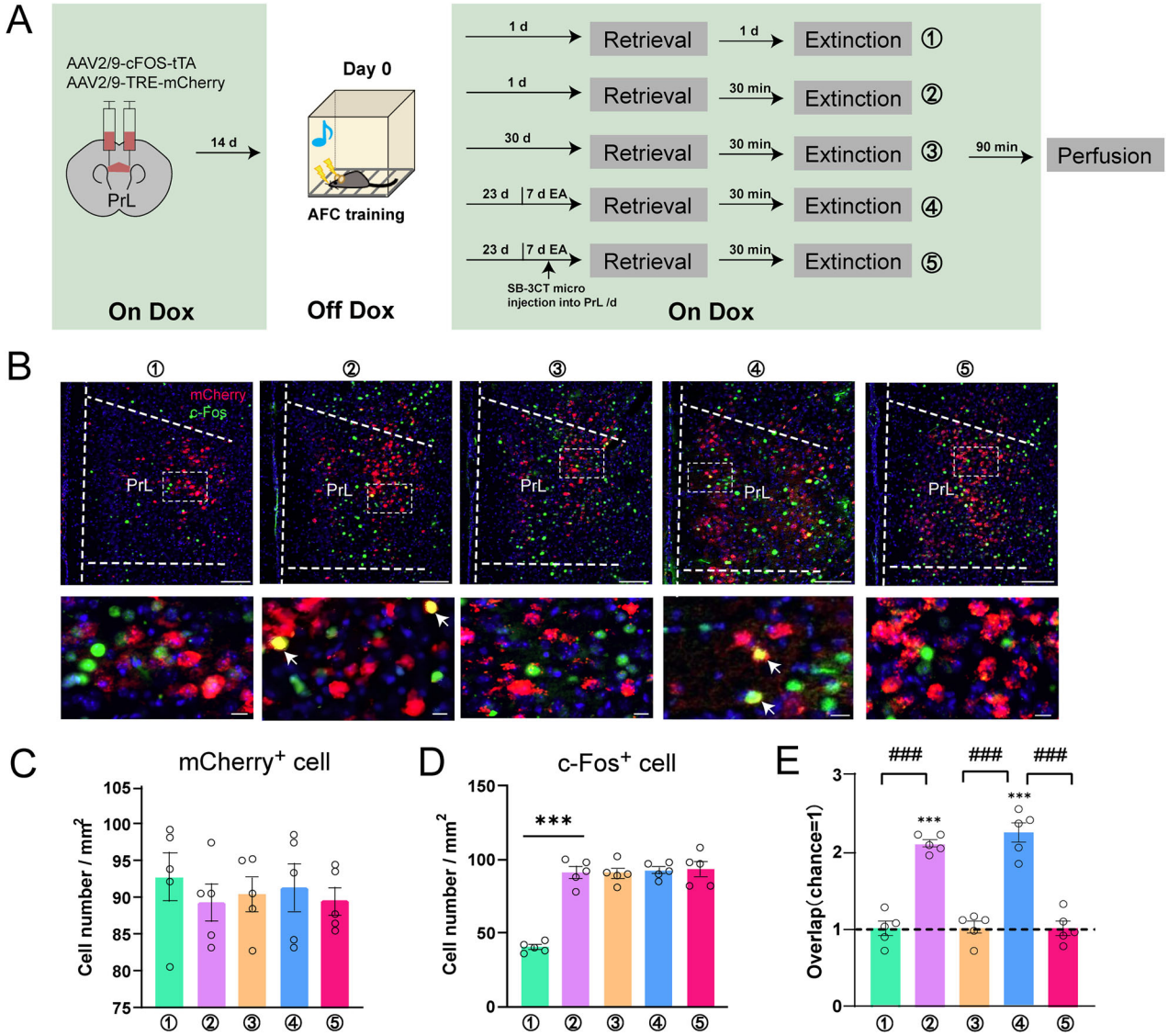


Fig. 6 EA enhances overlap between fear and extinction cells in the PrL during remote fear memory erasure. A Labeling strategy of fear engram cell by the inducible TetTag virus tool and the experimental design. **B** Representative images of mCherry^{+} (red) and c-Fos^{+} (green) immunofluorescence in PrL. The white arrow marked colabeled mCherry^{+}c-Fos^{+} cells. Scale bar, 200 μm (top), 20 μm (bottom). **C** Quantification of mCherry^{+} cell density in PrL. **D** Quantification of c-Fos^{+} cell density in PrL. **E** Quantification of overlap levels in PrL (paired t test, ***P < 0.001; one-way ANOVA with Tukey's multiple comparisons test, $^{###}$P < 0.001). Data are presented as mean ± SEM.

found that the overlap between fear and extinction cells in PrL of remote memory in R + E group showed no difference compared with chance level, which is consistent with that R + E paradigm could not erase remote memory and suggest that overlapping ensembles between fear and extinction cells play an essential role in memory updating. Interestingly, we found that the overlap of remote memory fear and extinction cells was increased in R + E with EA treatment group (Fig. 6B-E), in which the remote fear memory was effectively erased. What's more, the increased overlapping ensemble of remote memory was abolished by SB-3CT microinjection into PrL in R + E group with EA treatment (Fig. 6B-E). Thus, our results suggest that EA treatment facilitates the erasure of remote fear memory with increased overlapping ensemble between fear and extinction cells in the PrL via a MMP9 activity dependent mechanism.

DISCUSSION

How to erase long-lasting (remote) fear memory is a challenging question in fear related disorders treatment. We found significantly increased number of engram cells surrounded by PNNs in the PrL at 30 days compared with 1 day after fear conditioning. In addition, dissolving PNNs by ChABC treatment in the PrL facilitates R + E paradigm induced remote memory erasure. Electrocupuncture at Baihui and Neiguan significantly increase the MMP9 expression in PrL neurons, thus leading to the decreased levels of PNNs at remote time. Finally, similar as ChABC treatment, EA at Baihui and Neiguan promotes remote memory erasure, which was accompanied by the degradation of PNNs via BDNF-TrkB dependent signaling.

Our results provide several new insights into the effect and mechanism of EA on remote fear memory erasure. First, consistent with the previous report [10], we find post-retrieval extinction paradigm could not erasure remote memory in contrast to recent memory, which suggest that long-lasting (remote) fearful memories are more stable compared with recent memory. Memory engram cells referred to a population of neurons that are activated by learning, and must be reactivated for recall, where the memory information is supposed to be stored [27]. Interestingly, we found that compared with recent memory, the number of PNNs

surrounding engram cells in the PrL in the remote memory was significantly increased. PNNs are pericellular condensed extracellular matrix (ECM) structures and surround various types of neuron [18]. In the brain, the majority of neurons enveloped by PNNs are inhibitory fast spiking GABAergic parvalbumin-expressing (PV +) interneurons [31]. However, PNNs also surround subpopulations of excitatory glutamatergic neurons in different parts of the brain including cerebral cortex, amygdala and the CA2 region of the hippocampus [32–34]. To our knowledge, it is the first time to show that PNNs content surrounding engram cells in the PrL was significant increased as memory becomes long-term, which might explain in part the stability of remote memory since PNNs maintain a balance between the plasticity and stability of the synapses [17]. Indeed, it is recently reported that PNNs protect long-term memory by limiting activity-dependent inhibition from parvalbumin interneurons [26]. Removal of PNNs by ChABC could facilitate R + E induced remote memory erasure as comparable to recent memory, which further suggested that PNNs play an essential role in remote memory stability.

Recent study provided neuroanatomical explanation for the presence of acupoint specific pathway to transmit the peripheral stimulation into brain [35]. In an effort to investigate the effect of acupuncture on brain neuronal responses, the expression of c-Fos activity as an immediate early gene has been utilized to quantify brain neural activity [36]. We found that acupuncture at Baihui and Neiguan could dramatically increase the c-fos, Arc and BDNF expression in the PrL compared with sham group, which suggested that EA at Baihui and Neiguan could selectively increase the PrL activity. Based on previously reported thresholds for direct neuronal activation by electrical stimulation [37], we propose that our acupoint intervention might induce PrL activation via peripheral nerve to central nervous system transneuronal pathway, although the precise mechanistic pathway requires further investigation [35, 36]. Accompanying the neuronal activation, we found the PNNs contents were also decreased. To elucidate the mechanism underlying EA induced PNNs degradation, we measured the expression of MMP9 and ADAMTS after acupuncture treatment. We found Baihui and Neiguan EA treatment could induce the increased expression of MMP9 but not ADAMTS and renders remote memory to be erased by the R + E paradigm. In addition, microinjection of the MMP inhibitor SB-3CT into PrL could block EA treatment induced PNN degradation and memory erasure. Moreover, EA treatment also increased the levels of neuronal plasticity related proteins such as c-Fos, BDNF and Arc, which is consistent with that HDACi-supported remote memory updating led to increased neuroplasticity gene expression such as cFos, Arc, and Igf2 [10]. The levels of MMP proteins have been reported to be regulated by neural activity, sensory experiences, and during learning and memory processes and negatively correlated with the intensity of PNNs [19, 38, 39]. Our present studies found the TrkB antagonist K252a could block EA treatment induced PNN degradation and memory erasure. Thus, EA treatment might regulate fear engram cell plasticity in PrL through MMP9 regulated PNNs degradation via BDNF-TrkB signaling.

Memory updating represents a critical neurobiological mechanism through which organisms dynamically reorganize consolidated mnemonic schemas, enabling adaptive integration of novel environmental stimuli with pre-existing cognitive frameworks via synaptic reconfiguration and neural ensemble plasticity [11, 24]. The neural representation of memories, or engrams, is central to this process. It has been previous reported that increased engram overlap during memory linking which is one of the most extensively studied examples of memory updating [11, 24]. Memory engrams are dynamic, subject to modification or updating through processes such as reconsolidation, synaptic plasticity, and cellular reorganization [23]. Our laboratory was the first to identify a significant overlap between fear and extinction engrams during a post-retrieval paradigm, employing in vivo calcium imaging at the single-cell level in PrL [11]. We observed that the extent of overlap between fear engram cells and extinction engram cells was strongly correlated with memory erasure. In the present study, we found that the overlap between fear and extinction cells in the PrL during remote memory in the R + E group did not differ from chance levels, consistent with the inability of the R + E paradigm to erase remote memory. This suggests that the original fear engram cells in remote memory might show less plasticity compared with the fear engram cells in recent memory, which has been reported that engram cell overlap can be modulated their neuronal excitability [40, 41]. Interestingly, we observed that the overlap of fear and extinction cells in remote memory in the R + E with EA treatment group was significantly increased, which corresponded with effective erasure of remote fear memory. Furthermore, the increased overlap was abolished by SB-3CT microinjection into the PrL with EA treatment. These results provide evidence that EA treatment facilitates the erasure of remote fear memory by promoting an increased overlapping ensemble between fear and extinction cells in the PrL through an MMP9-dependent mechanism. Our current study gives the insight in regulating remote fear engram cells plasticity in PrL by EA via promoting PNN degradation.

In summary, the present study demonstrates that EA stimulation facilitates the erasure of remote memory by degrading PNNs through the upregulation of MMP9 expression. Additionally, PNNs contribute to the reorganization of PrL engram cells and keep the remote memory rigid. These findings suggest that EA may be an effective therapeutic intervention to erase remote pathological memories. Given that PTSD patients typically exhibit consolidated remote fear memories, post-retrieval extinction paradigms often fail to erase these memories without neuromodulatory interventions. Based on our results, electroacupuncture (EA), as a non-invasive approach, may facilitate the erasure of remote memory by targeting the PrL region. This finding could be further tested in human studies, providing support for future translational research for PTSD treatment. Future investigations into the neural circuit pathway that transduce peripheral acupuncture stimulation to PrL activation will shed light on enhancing the effect of EA on synaptic plasticity modulation in specific brain region.

DATA AVAILABILITY

Data are available upon request from the corresponding authors.

REFERENCES

1. Ressler KJ, Berretta S, Bolshakov VY, Rosso IM, Meloni EG, Rauch SL, et al. Post-traumatic stress disorder: clinical and translational neuroscience from cells to circuits. Nat Rev Neurol. 2022;18:273–88.
2. Richter-Levin G, Stork O, Schmidt MV. Animal models of PTSD: a challenge to be met. Mol Psychiatry. 2019;24:1135–56.
3. Bowers ME, Ressler KJ. An overview of translationally informed treatments for posttraumatic stress disorder: animal models of pavlovian fear conditioning to human clinical trials. Biol Psychiatry. 2015;78:E15–27.
4. de Quervain D, Schwabe L, Roozendaal B. Stress, glucocorticoids and memory:implications for treating fear-related disorders. Nat Rev Neurosci. 2017;18:7–19.
5. Tanner MK, Hake HS, Bouchet CA, Greenwood BN. Running from fear: exercise modulation of fear extinction. Neurobiol Learn Mem. 2018;151:28–34.
6. Monfils MH, Cowansage KK, Klann E, LeDoux JE. Extinction-reconsolidation boundaries: key to persistent attenuation of fear memories. Science. 2009;324:951–5.
7. Schiller D, Monfils MH, Raio CM, Johnson DC, Ledoux JE, Phelps EA. Preventing the return of fear in humans using reconsolidation update mechanisms. Nature. 2010;463:49–53.
8. Frankland PW, Bontempi B, Talton LE, Kaczmarek L, Silva AJ. The involvement of the anterior cingulate cortex in remote contextual fear memory. Science. 2004;304:881–3.
9. Inda MC, Muravieva EV, Alberini CM. Memory retrieval and the passage of time: from reconsolidation and strengthening to extinction. J Neurosci. 2011;31:1635–43.
10. Graff J, Joseph NF, Horn ME, Samiei A, Meng J, Seo J, et al. Epigenetic priming of memory updating during reconsolidation to attenuate remote fear memories. Cell. 2014;156:261–76.

11. Teng SW, Wang XR, Du BW, Chen XL, Fu GZ, Liu YF, et al. Altered fear engram encoding underlying conditioned versus unconditioned stimulus-initiated memory updating. Sci Adv. 2023;9:eadf0284.
12. Amorim D, Amado J, Brito I, Fiuza SM, Amorim N, Costeira C, et al. Acupuncture and electroacupuncture for anxiety disorders: a systematic review of the clinical research. Complement Ther Clin Pract. 2018;31:31–37.
13. Engel CC, Cordova EH, Benedek DM, Liu X, Gore KL, Goertz C, et al. Randomized effectiveness trial of a brief course of acupuncture for posttraumatic stress disorder. Med Care. 2014;52:S57–64.
14. Kim YD, Heo I, Shin BC, Crawford C, Kang HW, Lim JH. Acupuncture for posttraumatic stress disorder: a systematic review of randomized controlled trials and prospective clinical trials. Evid Based Complement Altern Med. 2013;2013:615857.
15. Li M, Li K, Zhang H, Jiang Y. Study on the mechanism of TMRK electroacupuncture in repairing synaptic plasticity in amygdala and hippocampus to relieve fear memory in PTSD rats. Technol Health Care. 2019;27:425–43.
16. Xue F, Xue SS, Liu L, Sang HF, Ma QR, Tan QR, et al. Early intervention with electroacupuncture prevents PTSD-like behaviors in rats through enhancing hippocampal endocannabinoid signaling. Prog Neuropsychopharmacol Biol Psychiatry. 2019;93:171–81.
17. Chelyshev YA, Kabdesh IM, Mukhamedshina YO. Extracellular matrix in neural plasticity and regeneration. Cell Mol Neurobiol. 2022;42:647–64.
18. Fawcett JW, Oohashi T, Pizzorusso T. The roles of perineuronal nets and the perinodal extracellular matrix in neuronal function. Nat Rev Neurosci. 2019;20:451–65.
19. Sorg BA, Berretta S, Blacktop JM, Fawcett JW, Kitagawa H, Kwok JC, et al. Casting a wide net: role of perineuronal nets in neural plasticity. J Neurosci. 2016;36:11459–68.
20. Lasek AW, Chen H, Chen WY. Releasing addiction memories trapped in perineuronal nets. Trends Genet. 2018;34:197–208.
21. Gogolla N, Caroni P, Luthi A, Herry C. Perineuronal nets protect fear memories from erasure. Science. 2009;325:1258–61.
22. Xue YX, Xue LF, Liu JF, He J, Deng JH, Sun SC, et al. Depletion of perineuronal nets in the amygdala to enhance the erasure of drug memories. J Neurosci. 2014;34:6647–58.
23. Josselyn SA, Tonegawa S. Memory engrams: recalling the past and imagining the future. Science. 2020;367:eaaw4325.
24. Yokose J, Okubo-Suzuki R, Nomoto M, Ohkawa N, Nishizono H, Suzuki A, et al. Overlapping memory trace indispensable for linking, but not recalling, individual memories. Science. 2017;355:398–403.
25. Li N, Teng SW, Zhao L, Li JR, Xu JL, Li N, et al. Carboxypeptidase e regulates activity-dependent trkb neuronal surface insertion and hippocampal memory. J Neurosci. 2021;41:6987–7002.
26. Shi W, Wei X, Wang X, Du S, Liu W, Song J, et al. Perineuronal nets protect long-term memory by limiting activity-dependent inhibition from parvalbumin interneurons. Proc Natl Acad Sci USA. 2019;116:27063–73.
27. Kitamura T, Ogawa SK, Roy DS, Okuyama T, Morrissey MD, Smith LM, et al. Engrams and circuits crucial for systems consolidation of a memory. Science. 2017;356:73–78.
28. Dwir D, Giangreco B, Xin L, Tenenbaum L, Cabungcal JH, Steullet P, et al. MMP9/RAGE pathway overactivation mediates redox dysregulation and neuroinflammation, leading to inhibitory/excitatory imbalance: a reverse translation study in schizophrenia patients. Mol Psychiatry. 2020;25:2889–904.
29. Zhang L, Gao YZ, Zhao CJ, Xia JY, Yang JJ, Ji MH. Reduced inhibitory and excitatory input onto parvalbumin interneurons mediated by perineuronal net might contribute to cognitive impairments in a mouse model of sepsis-associated encephalopathy. Neuropharmacology. 2023;225:109382.
30. Kuzniewska B, Rejmak E, Malik AR, Jaworski J, Kaczmarek L, Kalita K. Brain-derived neurotrophic factor induces matrix metalloproteinase 9 expression in neurons via the serum response factor/c-Fos pathway. Mol Cell Biol. 2013;33:2149–62.
31. Carulli D, Pizzorusso T, Kwok JC, Putignano E, Poli A, Forostyak S, et al. Animals lacking link protein have attenuated perineuronal nets and persistent plasticity. Brain. 2010;133:2331–47.
32. Lensjo KK, Christensen AC, Tennoe S, Fyhn M, Hafting T. Differential expression and cell-type specificity of perineuronal nets in hippocampus, medial entorhinal cortex, and visual cortex examined in the rat and mouse. eNeuro. 2017;4:ENEURO.0379–16.2017.
33. Morikawa S, Ikegaya Y, Narita M, Tamura H. Activation of perineuronal net-expressing excitatory neurons during associative memory encoding and retrieval. Sci Rep. 2017;7:46024.
34. Wegner F, Hartig W, Bringmann A, Grosche J, Wohlfarth K, Zuschratter W, et al. Diffuse perineuronal nets and modified pyramidal cells immunoreactive for glutamate and the GABA(A) receptor alpha1 subunit form a unique entity in rat cerebral cortex. Exp Neurol. 2003;184:705–14.
35. Liu S, Wang Z, Su Y, Qi L, Yang W, Fu M, et al. A neuroanatomical basis for electroacupuncture to drive the vagal-adrenal axis. Nature. 2021;598:641–5.
36. Chu WG, Zhang R, Li HT, Li YC, Ding H, Li ZZ, et al. Locus coeruleus noradrenergic-spinal projections contribute to electroacupuncture-mediated antinociception in postoperative pain in mice. Adv Sci. 2025;12:e01182.
37. Voroslakos M, Takeuchi Y, Brinyiczki K, Zombori T, Oliva A, Fernandez-Ruiz A, et al. Direct effects of transcranial electric stimulation on brain circuits in rats and humans. Nat Commun. 2018;9:483.
38. Duncan JA, Foster R, Kwok JCF. The potential of memory enhancement through modulation of perineuronal nets. Br J Pharmacol. 2019;176:3611–21.
39. Sanchez B, Kraszewski P, Lee S, Cope EC. From molecules to behavior: Implications for perineuronal net remodeling in learning and memory. J Neurochem. 2024;168:1854–76.
40. Choucry A, Nomoto M, Inokuchi K. Engram mechanisms of memory linking and identity. Nat Rev Neurosci. 2024;25:375–92.
41. Zhou Y, Won J, Karlsson MG, Zhou M, Rogerson T, Balaji J, et al. CREB regulates excitability and the allocation of memory to subsets of neurons in the amygdala. Nat Neurosci. 2009;12:1438–43.

ACKNOWLEDGEMENTS

This study was supported by the STI2030 Major Projects (2021ZD0202804 to Zhe-Yu Chen), National Natural Science Foundation of China (No. 82441051 and 32171029 to Zhe-Yu Chen, 32400851 to Shuai-Wen Teng), the Key R&D Program of Shandong Province (2022ZLGX03 to Zhe-Yu Chen), a postdoctoral innovation project of Shandong Province (SDCX-ZG-202400143 to Shuai-Wen Teng). We thank Translational Medicine Core Facility of Shandong University and Research Center for Basic Medical Sciences of Qilu Hospital affiliated to Shandong University for consultation and instrument availability that supported this work.

AUTHOR CONTRIBUTIONS

This study was conceptualized and designed by ZYC and SWT SWT and WBG carried out the experiments and analyzed data. YZH, BFS and SBG contributed to transgenic mice keeping, histology staining, western blot and quantification. KYW and WL contributed to the behavioral experiment. The paper was written and edited by ZYC, SWT and WBG.

COMPETING INTERESTS

The authors declare no competing interests.

ETHICS APPROVAL AND CONSENT TO PARTICIPATE

All methods were performed in accordance with the relevant guidelines and regulations. All animal experiments were approved by the Institutional Animal Care and Use Committee (IACUC) of Shandong University (ECSBMSSDU2021-2-111).

ADDITIONAL INFORMATION

Supplementary information The online version contains supplementary material available at https://doi.org/10.1038/s41398-025-03789-3.

Correspondence and requests for materials should be addressed to Zhe-Yu Chen.

Reprints and permission information is available at http://www.nature.com/reprints

Publisher's note Springer Nature remains neutral with regard to jurisdictional claims in published maps and institutional affiliations.

Open Access This article is licensed under a Creative Commons Attribution-NonCommercial-NoDerivatives 4.0 International License, which permits any non-commercial use, sharing, distribution and reproduction in any medium or format, as long as you give appropriate credit to the original author(s) and the source, provide a link to the Creative Commons licence, and indicate if you modified the licensed material. You do not have permission under this licence to share adapted material derived from this article or parts of it. The images or other third party material in this article are included in the article's Creative Commons licence, unless indicated otherwise in a credit line to the material. If material is not included in the article's Creative Commons licence and your intended use is not permitted by statutory regulation or exceeds the permitted use, you will need to obtain permission directly from the copyright holder. To view a copy of this licence, visit http://creativecommons.org/licenses/by-nc-nd/4.0/.

© The Author(s) 2025